

Satellite Sub-Pixel Rainfall Variability

ERIC W. HARMSEN¹
SANTA ELIZABETH GOMEZ MESA²
EDVIER CABASSA³
NAZARIO D. RAMÍREZ-BELTRAN⁴
SANDRA CRUZ POL⁵
ROBERT J. KULIGOWSKI⁶
RAMÓN VASQUEZ⁷

¹Department of Agricultural and Biosystems Engineering, University of Puerto Rico
P.O. Box 9030, Mayagüez, PR 00681,
U.S.A.
eharmsen@uprm.edu

²Department of Mathematics, University of Puerto Rico,
P.O. Box 9030, Mayagüez, PR 00681,
U.S.A.
santagm3@gmail.com

³Department of Computer and Electrical Engineering, University of Puerto Rico
P.O. Box 9040, Mayagüez, PR 00681,
U.S.A.
ecabassa@gmail.com

⁴Department of Industrial Engineering, University of Puerto Rico
P.O. Box 9030, Mayagüez, PR 00681,
U.S.A.
nazario@ece.uprm.edu

⁵Department of Computer and Electrical Engineering, University of Puerto Rico,
P.O. Box 9040, Mayagüez, PR 00681,
U.S.A.
SandraCruzPol@ieee.org

⁶NOAA/NESDIS Center for Satellite Applications and Research (STAR)
5200 Auth Rd., Camp Springs, MD 20746-4304
U.S.A.
Bob.Kuligowski@noaa.gov

⁷Department of Computer and Electrical Engineering, University of Puerto Rico
P.O. Box 9040, Mayagüez, PR 00681,
U.S.A.
reve@ece.uprm.edu

Abstract: - Rain gauge networks are used to calibrate and validate quantitative precipitation estimation (QPE) methods based on remote sensing, which may be used as data sources for hydrologic models. The typical approach is to adjust (calibrate) or compare (validate) the rainfall in the QPE pixel with the rain gauge located within the pixel. The QPE result represents a mean rainfall over the pixel area, whereas the rainfall from the gauge represents a point, although it is normally assumed to represent some area. In most cases the QPE pixel area is millions of square meter in size. We hypothesize that some rain gauge networks in environments similar to this study (i.e., tropical coastal), which provide only one rain gauge per remote sensing pixel, may lead to error when used to calibrate/validate QPE methods, and that consequently these errors may be propagated throughout hydrologic models. The objective of this paper is to describe a ground-truth rain gauge network located in western Puerto Rico which will be available to test our hypothesis. In this paper we discuss observations from the rain gauge network, but do not present any QPE validation results. In addition to being valuable for validating satellite and radar QPE data, the rain gauge network is being used to test and calibrate atmospheric simulation models and to gain a better understanding of the sea breeze effect and its influence on rainfall.

In this study, a large number of storms (> 60) were evaluated between August 2006 and August 2008. The area covered by the rain gauge network was limited to a single GOES-12 pixel (4 km x 4 km). Five-minute and total storm rainfall amounts were spatially variable at the sub-pixel scale. The average storm rainfall from 20% of the 120 possible rain gauge-pairs was found to be significantly different at the 5% of significance level, indicating significant rainfall variation at the sub-pixel scale. The average coefficient of determination (r^2), describing the goodness of fit of a linear model relating rain gauge pairs, was 0.365, further suggesting a significant degree of variability at the satellite sub-pixel scale. Although there were several different storm types identified (localized, upper westerly trough, tropical easterly wave, tropical westerly trough, cold front and localized with cold front), there did not appear to be any relationship between storm type and the correlation patterns among the gauges.

Key-Words: - satellite pixel, rainfall variability, QPE, rain gauge, radar, validation, hydrologic modeling

1 Introduction

It is commonly assumed that a single rain gauge located within a QPE pixel represents the average rainfall for the pixel area (e.g., [1] and [2]). The National Oceanic and Atmospheric Administration's (NOAA) Hydro Estimator (HE) algorithm [3], which utilizes data from the GOES geostationary satellite to estimate rainfall, for example, has an approximate pixel size of 4 km x 4 km (16,000,000 m²), compared to a cross-sectional area of roughly 0.032 m² for the standard National Weather Service tipping bucket gauge. The National Weather Service's (NWS) Next Generation Radar (NEXRAD) estimates rainfall within a radial coordinate system (base resolution 2 to 4 km), in which the pixel size increases with distance from the radar antenna [4]. NEXRAD accuracy also decreases with distance from the antenna owing to the curvature of the earth and in some cases the presence of obstructions (e.g., mountains); additional details can be found in [5]. The differences in temporal and spatial scales make the comparison of QPE methods with ground-based rain gauges difficult [6]. Other potential sources of error include rain gauge inaccuracy, assumptions made in the development of the QPE algorithm that may be violated under local (e.g., tropical) rainfall conditions, and navigation errors in the satellite pixel coordinates. For example, the navigation errors of the GOES-12 pixels at nadir are on the order of 4-6 km [7].

Hydrologic models used to estimate storm hydrographs and flood levels and extent may be sensitive to rainfall distribution at the QPE sub-pixel scale [8]. Bevan and Hornberger [9] have stated that "... an accurate portrayal of spatial variation in rainfall is a prerequisite for accurate simulation of stream flows". Spatial rainfall variability greatly affects runoff processes in watersheds [10]. Goodrich [11] has stated that rainfall runoff accuracy will increase with an increasing number of rain gauges in the watershed, which will improve the representation of the spatial characteristics of rainfall. Rainfall estimates at a point differ from catchment averages because rainfall varies spatially and its spatial distribution over the catchment determines the amount of rainfall that is integrated in time and space [12]. Moreiraa et al. [10] evaluated rainfall spatial variability effects on catchment runoff. The study area was a 2.1 km² catchment in northeastern Brazil. The catchment response of the relatively small catchment area was quite sensitive to the occurrence of rainfall with high spatial variability. Bell and Moore [13] evaluated the sensitivity of simulated runoff using rainfall data from gauges and radar. The rain gauge system consisted of 49 gauges over the 135 km² Brue catchment in southwestern England. They evaluated convective and stratiform rainfall events. Runoff variability was strongest during convective storm events and weakest during stratiform events. Surprisingly, the authors obtained the best performance using lower-

resolution rainfall data and a lower-resolution hydrologic model. This result was attributed to the fact that the original model was calibrated with lower resolution data. Hydrologic models need to be recalibrated when rainfall of a different resolution is used.

Numerous small-scale rainfall variation studies have been conducted (e.g., [10], [14], [15]). For instance, Bidin and Chappell [14] evaluated rainfall variation for differing wind fields with 46 rain gauges within a 4 km² rainforest in Northeastern Borneo. They observed a very high degree of spatial variability. Seasonal totals were correlated with gauge separation distance, aspect and topographic relief. Changes in rainfall patterns over the 4 km² catchment were related to complex local topographic effects in the regional wind field. Goodrich et al. [15] studied small scale rainfall variability within a 4.4 ha area in the semiarid USDA Walnut Gulch Experimental (WGE) Watershed in Arizona, USA. The average observed rainfall gradient was 1.2 mm/100 m. They concluded that the assumption of rainfall uniformity in convective environments similar to the WGE Watershed is invalid. Krajewski et al. [16]) compared rain gauges in Guam at three time scales (5, 15, and 60 min) and three spatial scales (1, 600, and 1100 m). The largest variations occurred for the smallest time scale and the largest spatial scale. The smallest variations occurred for the largest time scale and the smallest spatial scale.

We hypothesize that many rain gauge networks in environments similar to this study (i.e., tropical coastal), which provide only one rain gauge per remote sensing pixel, may be inadequate to calibrate/validate QPE methods, and that consequently QPE data may be inadequate to use with hydrologic models. The objective of this paper is to present results from a rain gauge network that will be used to validate several QPE methods (e.g., GOES Hydro-Estimator [3], SCaMPR [17], NEXRAD and the University of Puerto Rico Collaborative Adaptive Sensing of the Atmosphere radar network). Implications of the results on calibration/validation of QPE methods are discussed.

2 Methodology

During July 2006, sixteen tipping bucket rain gauges (Spectrum Technology, Inc.¹) were installed within the area covered by one GOES pixel, with the objective of comparing to the operational National Environmental Satellite, Data, and Information Service (NESDIS) Hydro-Estimator algorithm [18]. Each rain gauge is

equipped with a data logger capable of storing rainfall depth every 5 minutes over a 24-day period. The study area was located near to the University of Puerto Rico's Mayagüez Campus (UPRM) in western Puerto Rico (Fig. 1). The pixel area of 4 km x 4 km (16 km²) was divided into sixteen evenly spaced squares of 1 km² each. To locate the rain gauges the following steps were used:

1. The center points of the GOES pixels were obtained from NESDIS.
2. An appropriate GOES pixel was selected, which included a relatively large range of topographic relief east of the Mayagüez Bay in western Puerto Rico.
3. Using ArcGIS, sixteen points were located (evenly spaced) within the GOES pixel.
4. With the assistance of a ground positioning system (GPS), properties (mainly residential) were located which were as close as possible to the center point locations identified in step no. 3. In each case it was necessary to obtain permission from the property owner before installing the rain gauges.
5. The actual coordinates of the installed rain gauges were recorded and entered into ArcGIS (Fig. 2).

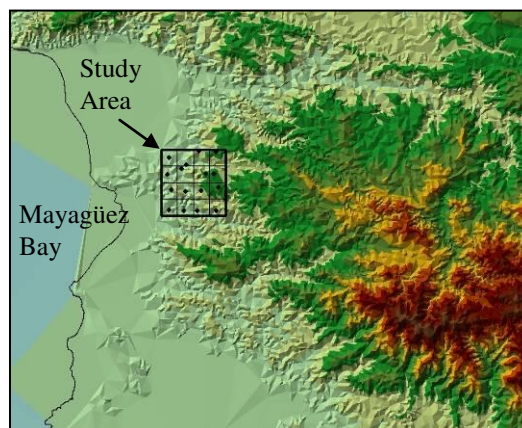


Figure 1. Study area in western Puerto Rico corresponding to a GOES pixel (4 km x 4 km). Colors represent variations in topography.

¹ Reference to a commercial product in no way constitutes an endorsement of the product by the authors.

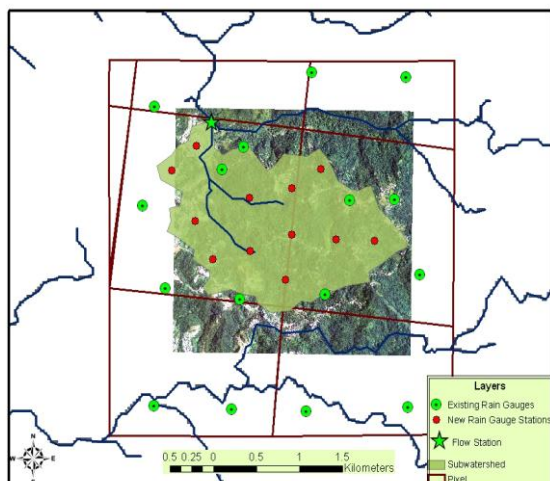


Figure 2. Twenty-eight tipping bucket rain gauges used in the study. The 12 rain gauges installed in June of 2007 were distributed within a subwatershed of the Añasco River.

Some of the rain gauges could not be located close to the center points of the squares because of a lack of access—generally to undeveloped valleys. Consequently the final locations of rain gauges were not evenly spaced; however, this resulted in producing a random (possibly beneficial) aspect to the locations of rain gauges within each sub-area.

The data logger clocks were synchronized and programmed to record cumulative rainfall depth every 5 minutes. All rain gauges were placed in areas free from obstructions. It was necessary to locate a few of the gauges on roof tops (approximately 5 meters above the ground) owing to inappropriate conditions on the ground. An effort was made to level each of the rain gauges to assure proper functioning.

In June of 2007, another 12 tipping bucket rain gauges were added to the network. These rain gauges were distributed within a subwatershed of the Añasco River for future hydrologic evaluation. Figure 2 shows the location of the 12 rain gauges within the subwatershed and the location of a stream gauge (Solinst Levelogger) installed at the outlet of the subwatershed. It should be noted that to maintain consistency in this study, only the original 16 rain gauges were used in the statistical analysis.

Storm data were collected for 62 storms between August 2006 and August 2007. The storm data collected included: start and end times, storm duration, number of operational rain gauges (n), average total storm rainfall, standard deviation, and maximum and minimum rain gauge amounts. Storms were classified according to whether they were locally formed by sea breezes and heating, or generated by large weather

systems of either easterly or westerly origin. For this it was necessary to gather supplementary information on the synoptic weather conditions, and the local pattern and timing of convection near Mayagüez, Puerto Rico. Supplementary information included large scale maps of upper winds and precipitable water, visible or IR satellite and radar images, and radiosonde profiles at San Juan. The types of weather systems observed were:

- Localized = isolated over western Puerto Rico with trade wind convergence
- Tropical westerly trough = southwesterly moist flow and SW-NE cloud bands
- Tropical easterly wave = deep easterly flow with widespread cloudiness
- Upper westerly trough = westerly flow in mid-levels coming down from north
- Cold front = frontal cloud band penetrating from Florida

The Kolmogorov-Smirnov (K-S) test [19] was used to evaluate normality of the non-transformed and log-transformed storm totals for each of the rain gauges for 90 storms between August 2006 and August 2008. In the case of the non-transformed data, not one of the 16 data sets was determined to be normal. In the case of the log-transformed data, eleven of the sixteen data sets were determined to be normally distribution. Therefore, two non-parametric comparison tests were used which do not require that the data come from a normal distributions. The two tests used were the Mann-Whitney [20] and Wilcoxon [21] signed-rank tests. The purpose of these two tests is to assess whether two samples of observations come from the same distribution. If the analysis results in a small probabilities (e.g., ≤ 0.05) then the null hypothesis must be rejected, that is to say that the two samples are significantly different. A Pearson correlation table was also generated for the sixteen data sets. All statistical analyses were performed using the computer software StatMost32 [22].

The reason for conducting the significant difference tests was based on the following rationale. QPE methods based on remote sensing usually compare (or adjust) the remotely sensed rainfall estimate based on a single rain gauge located within the remotely sensed pixel. The rain gauge, in virtually all cases, will be randomly located within the pixel (as opposed to, for example, being located at the pixel center). This is because the entity that manages the satellite or radar is typically different than the entity that installed the rain gauges. If there is a large amount of sub-pixel rainfall variation then the QPE will be compared with a rain gauge that does not represent other locations within the pixel. On the other hand, if there is no significant difference between randomly located pairs of rain gauges, then this would suggest that the sub-pixel

variability is low and the QPE can be compared (or adjusted) to rain gauges located at any location within the pixel.

3 Results

As an example of the measured rainfall data, Fig. 3 shows the depth of rainfall measured every 5 minutes by sixteen rain gauges on 6 August 2006. Figure 4a shows the spatial distribution of total rainfall for the same storm. It is clear that the rainfall can vary significantly within the satellite pixel area. The average and standard deviation for the rainfall were 30.8 mm and 13.6 mm, respectively, while the maximum and minimum recorded rainfall were 55.6 mm and 9.2 mm, respectively. In addition to 6 August 2006 (4a), Fig. 4 shows the rainfall variation for storms occurring on 16 August (4b), 18 August (4c) and 22 October (4d), 2006. For these storms, the maximum rainfall gradients were 20.4, 56.9, 55, and 65 mm/km, respectively. Spatial variation in rainfall distribution as shown in Fig. 4 is commonly observed during the “wet” season (August through November) in western Puerto Rico.

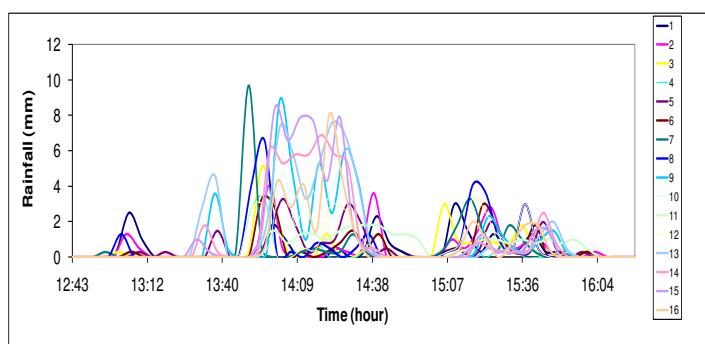


Figure 3. Rainfall measured from rain gauges on August 6th, 2006. Numbers 1-16 in the legend represent the rain gauge number.

Table 1 lists the statistics associated with 62 storms which occurred between August 2006 and August 2007. The table includes storm type, number for of storms, average storm start and end times, average storm durations, average number of operational rain gauges (n), average total storm rainfall, average standard deviation, average maximum and average minimum rain gauge amounts. The overall average for each of the parameters is presented at the bottom of Table 1. On average, the rain storms started at 15:02 and ended at 17:22, with an average duration of 2.33 hours. The average, maximum, and minimum rainfall depths were 15.94 mm, 30.14 mm and 4.53 mm, respectively.

The distribution of the storm classifications were as follows (Table 1): localized = 22 cases, upper westerly trough = 16 cases, tropical easterly wave = 11 cases, cold front = 6 cases, tropical westerly trough = 6

cases, and localized with cold front = 1. These results indicate the importance of the localized sea-breeze induced storm to the local hydrology. The average rainfalls produced from each type of storm were 15.4 mm, 14.4 mm, 17.2 mm, 9 mm, 27.03 mm and 13.64 for localized, upper westerly trough, tropical easterly wave, cold front, storms tropical westerly trough, and localized with cold front, respectively.

In mid-June 2007, 12 additional rain gauges were added within a small subwatershed located within the 4 km x 4 km pixel as shown in Fig. 2. Fig. 5 shows the variation in 5 minute rainfall at four different times (14:27, 14:37, 15:32 and 16:22) on 27 June 2007. Large variations can be observed between the individual 5 minute intervals.

Table 2 shows the results of the statistical comparison of all possible pairs of the sixteen rain gauge data sets (green circles in Figure 2) derived from 90 storms between August 2006 and August 2008; however data from all the rain gauges were not available for all 90 storms. For example, there were 77 rainfall totals available for rain gauge no. 7. Rain gauge no. 8 had the smallest data set with only 23 rainfall totals. The main reason that data were not available for all storms was the lack of measurement of rainfall by a rain gauge (i.e., rainfall measured was zero). Because we could not be certain that this was real or if the rain gauge became plugged with debris, for example, all zero rainfall values were discarded. It should be noted that the decision to discard this data will result in data sets that may underestimate the variability of rainfall. Therefore, in the statistical analysis presented below it should be kept in mind that our assessment of variability is conservatively low, because without a doubt, some of the discarded zero rain gauge values were in fact correct.

For the Mann-Whitney and the Wilcoxon analyses (log-transformed and non-transformed data), 17 to 25% (20.9% mean) of average rainfall totals for all rain gauge pairs were significantly different (Table 2). A Pearson Correlation Table (Dataxiom Software, Inc., 2001) was generated for the sixteen data sets (not shown) and the overall average correlation coefficient (r) was 0.60. Pearson correlation indicates the strength of a linear relationship between two variables. The coefficient of determination (r^2) can be estimated by taking the square of r , which in this case yielded $r^2 = 0.37$. Therefore, on average a linear model can explain 36.5% of the variance between two randomly selected rain gauge data sets. This is quite a low coefficient of determination, and is another indication of rainfall variability at the satellite sub-pixel scale. Figures 6 and 7 show the frequency and cumulative frequency of r and r^2 , respectively, for the 16 rain gauge pairs. Of the 120 r^2 values, 90% were less than 0.7, 67% were less than 0.5, and 30% were less than 0.2.

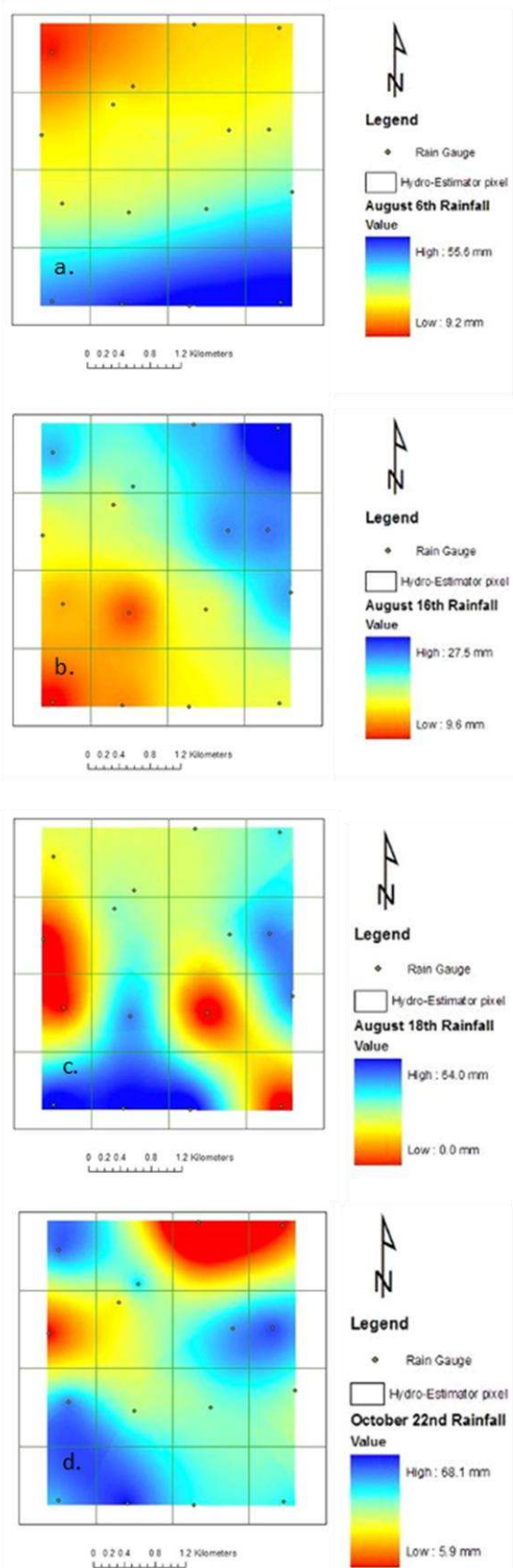


Figure 4. Spatial distribution of rainfall for storms on 6 August (a), 16 August (b), 18 August (c) and 22 October (d), 2006.

Figure 8 shows the upper 95% confidence interval (CI_U) minus the lower 95% confidence interval (CI_L) for the mean gauge rainfall for the 90 storms. $CI_U - CI_L$ provides another indication of how variable the data is with respect to the mean rain gauge data. The average $CI_U - CI_L$ was 15.6 mm (0.6 inches), while the maximum $CI_U - CI_L$ was 87.7 mm (3.5 inches). Ironically, with such a large range between the upper and lower 95% confidence limits, it may be relatively easy to obtain a QPE which falls within this range. What these results indicate is that we do not know what the mean rainfall is with a high degree of certainty.

4 Discussion

Typically QPE methods are compared with existing rain gauge networks. For example, Cruz Gonzalez [1] compared the HE algorithm with an existing U.S. Geological Survey rain gauge network in Puerto Rico (125 rain gauges). If we were to superimpose the QPE pixels over the area of the island, for example the HE method having a pixel resolution of 4 km x 4 km, the individual rain gauge would fall at some random location within an HE pixel. As Figs. 4 and 5 illustrate, a large difference could be obtained depending upon where the rain gauges were located within the pixels. Statistically speaking, one out of every five rain gauges would not be representative of the rainfall occurring at other locations within the pixel. This problem is reduced when averaging estimates over time, but is most acute for short-term estimates within a single storm [15]—the type of data needed for real-time hydrologic flood forecasting [23, 24].

5 Summary and Conclusion

The purpose of this study was to evaluate the spatial rainfall variability within a QPE pixel (4 km x 4 km HE pixel) in a tropical watershed located in western PR. Graphical data were presented for four storms (total storm rainfall), several 5-minute intervals within a single storm on 27 June 2007, and tabular data were presented for 62 storms. Rainfall was observed to be variable within the 4 km x 4 km study area. Average storm rainfall from more than one fifth (20.9%) of the 120 rain gauge-pairs evaluated for 90 storms, based on non-parametric statistics, were significantly different at the 5% of significance level, indicating significant rainfall variation at the sub-pixel scale. The overall coefficient of determination was 0.37. Of the 120 r^2 values, 90% were less than 0.7, 67% were less than 0.5, and 30% were less than 0.2. The average $CI_U - CI_L$ was 15.6 mm (0.6 inches), while the maximum $CI_U - CI_L$ was 87.7 mm.

Results from this study clearly illustrate that for existing rain gauge networks (e.g., USGS) used in environments similar to this study (i.e., coastal tropical), significant sub-pixel variation can be expected. In these cases, where a single rain gauge exists within the QPE pixels and is used to either calibrate or validate a remotely sensed QPE method, error may be introduced into the QPE, and may be propagated through any hydrologic model used. The practical consequences of this error propagation are that the hydrologic parameters derived as part of the hydrologic model calibration will be incorrect.

6 Acknowledgement

Financial support was received from NOAA-CREST, NSF-CASA, NASA-IDEAS, USDA HATCH (H-402) and USDA-TSTAR (100). Thanks to Dr. Mark Jury of the University of Puerto Rico-Mayagüez for assistance with determining storm classifications, and to Dr. Raúl Macchiavelli for his advice on the statistical approach used in this study. Thanks also to the students that helped install rain gauges and collect rainfall data: Jerak Cintrón, Ian García, Mariana León Pérez, Melvin Cardona, Ramón Rodríguez, Marcel Giovanni Prieto, Víctor Hugo Ramírez, Yaritza Pérez, Romara Santiago, Alejandra Roja, Jorge Canals, Julian Harmsen and Lua Harmsen.

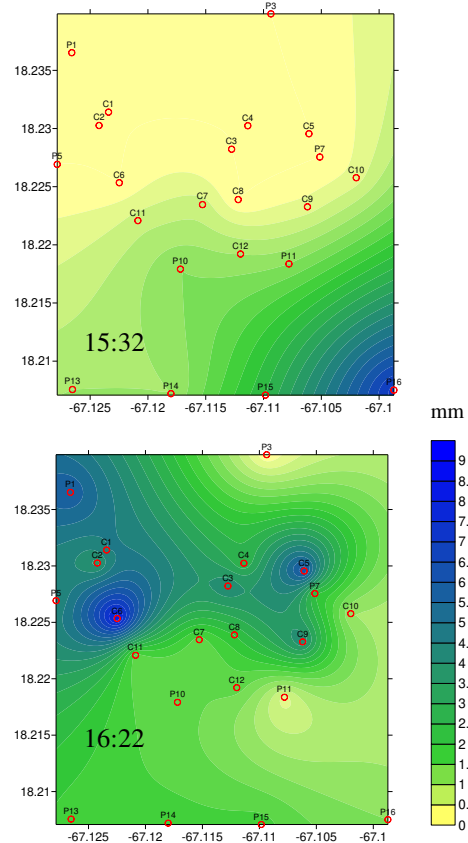


Figure 5. Spatial distribution of 5-minute rainfall values (mm) at 14:27, 14:37, 15:32 and 16:22 hours, for a storm occurring on 27 June, 2007.

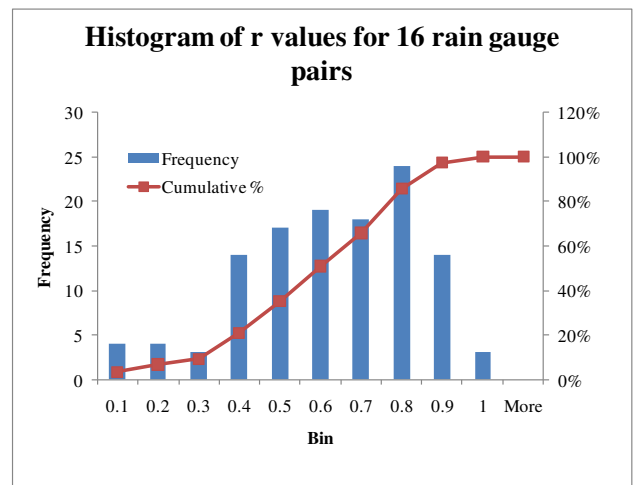
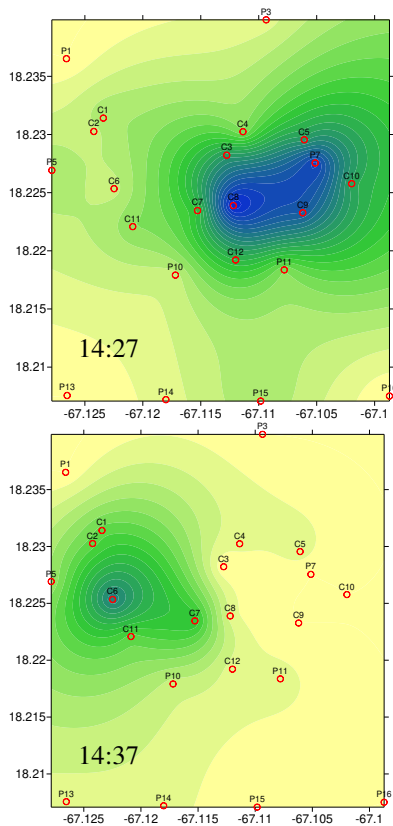


Figure 6. Frequency and cumulative frequency of correlation coefficients (r) for 16 rain gauge pairs.

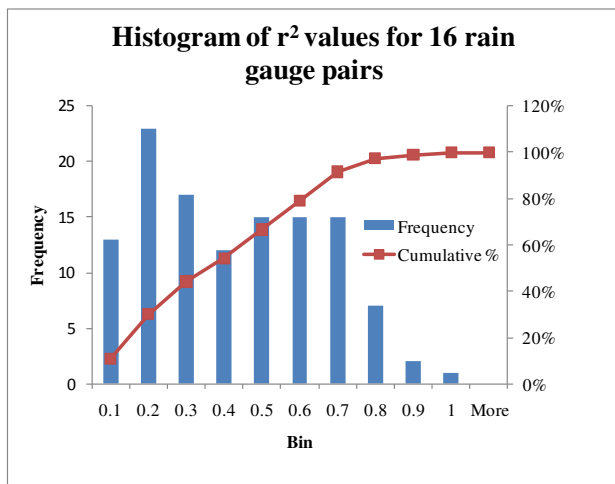


Figure 7. Frequency and cumulative frequency of coefficient of determination (r^2) for 16 rain gauge pairs.

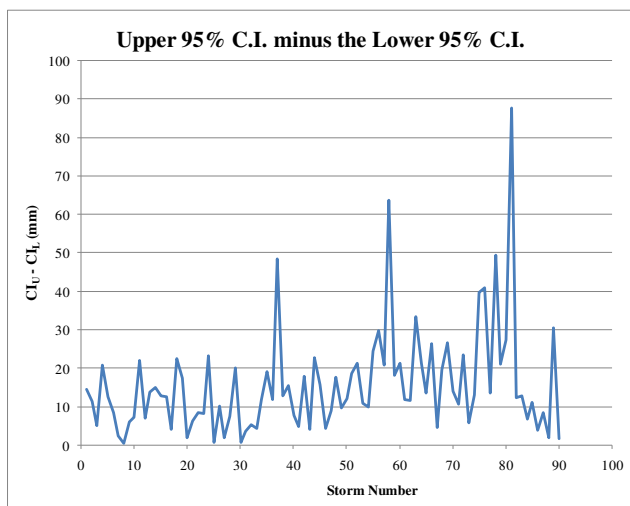


Figure 8. Upper 95% confidence interval (CI_U) minus the lower 95% confidence interval (CI_L) for 90 storms.

References:

- [1] Cruz Gonzalez, B., 2006: Validacion del Algoritmo Hidro-Estimador en la Region de Puerto Rico (Validation of the Hydro-Estimador Algorithm in the Puerto Rico Region). Tesis Departamento de ININ, Universidad de Puerto Rico Mayagüez.
- [2] Vila D. and I. Velasco, 2002. Some experiences on satellite rainfall estimation over South America. Proceedings, 1st International Precipitation Working Group (IPWG) Workshop Madrid, Spain.
- [3] Scofield, R.A. and R.J. Kuligowski, 2003: Status and outlook of operational satellite precipitation algorithms for extreme-precipitation events. *Wea. Forecasting*, 18, 1037-1051.
- [4] Beringer D.B. and J.D. Ball, 2004: The Effects of NexRad Graphical Data Resolution and Direct Weather Viewing on Pilots' Judgments of Weather Severity and Their Willingness to Continue a Flight. DOT/FAA/AM-04/5. [Available from the Office of Aerospace Medicine, F.A.A. 800 Independence Ave. SW Washington, DC 20591.]
- [5] Young, C. B., B. R. Nelson, A. A. Bradley, J. A. Smith, C. D. Peters-Lidard, A. Kruger, and M. L. Baeck, 1999: An evaluation of NEXRAD precipitation estimates in complex terrain. *J. Geophys. Res.*, 104(D16), 19691-19703.
- [6] Kuligowski, R. J. 1997: An overview of the National Weather Service quantitative precipitation estimates. TDL Office Note 97-4, NOAA/NWS/MDL, 28 pp. [Available at <http://www.nws.noaa.gov/im/pub/tdl97-4.pdf>.]
- [7] Hilger, D. W., and T. J. Schmit, 2007: An overview of the GOES-13 Science Test. Preprints, 3rd Symp. on Future National Operational Environmental Satellites, San Antonio, Amer. Meteor. Soc., CD-ROM, P1.31
- [8] Gioia, A. V. Iacobellis, S. Manfreda and M. Fiorentino, 2007. Climate and soil controls on flood frequency. Proceedings of the 2nd IASME / WSEAS International Conference on Water Resources, Hydraulics & Hydrology, Portoroz, Slovenia, May 15-17, 2007. Pgs. 82-89.
- [9] Bevan, K.J. and G.M. Hornberger, 1982: Assessing the effect of spatial pattern of precipitation in modeling stream flow hydrographs. *Water Resour. Bull.*, 18, 823-829.
- [10] Moreiraa L.F.F., A. M. Righetto, and V. M. Medeiros, 2006: Uncertainty analysis associated with rainfall spatial distribution in an experimental semiarid watershed, Northeastern Brazil. Preprints, 3rd Biennial Meeting of the International Environmental Modelling and Software Society, Burlington, VT.
- [11] Goodrich, D.C., 1990: Geometric simplification of a distributed rainfall-runoff model over a range of basin scales. Ph. D. Dissertation. University of Arizona. Tucson, AZ.
- [12] Vieux, B.E. and P.B. Bedient. 1998: Estimation of rainfall for flood prediction from WSR-88D reflectivity: A case study, 17-18 October 1994. *Wea. Forecasting*, 13, 507-513.

- [13] Bell, V.A. and R. J. Moore, 2000: The sensitivity of catchment runoff to rainfall data at different spatial scales. *Hydrol. Earth System Sci.*, 4, 653-667.
- [14] Bidin, K. and N. A. Chappell, 2003. First evidence of a structured and dynamic spatial pattern of rainfall within a small humid tropical catchment. *Hydrology and Earth System Sciences*, 7(2), 245-253.
- [15] Goodrich, D. C, J.M. Faures, D.A. Woolhiser, L.J. Lane, and S. Sorooshian. 1995: Measurement and analysis of small-scale convective storm rainfall variability. *J. Hydrol.* 173 (1-4), 283-308.
- [16] Krajewski, W. F., G.J. Ciach and E. Habib, An analysis of small-scale rainfall variability in different climatic regimes, *Hydrol. Sci. J.* 48 (2003), pp. 151–162.
- [17] Kuligowski, R. J., 2002: A self-calibrating GOES rainfall algorithm for short-term rainfall estimates. *J. Hydrometeor.*, **3**, 112-130.
- [18] Kuligowski, R. J., 2004. Re-calibrating the operational Hydro-Estimator satellite precipitation algorithm. 13th Conference on Satellite Meteorology and Oceanography. 20-23 September, 2004. Norfolk, VA.
- [19] Steel, R. G. D. and J. H. Torrie, 1980. *Principles and Procedures of Statistics A Biometrical Approach*, Second Edition. McGraw-Hill Book Company, pp 633.
- [20] Mann, H. B., & Whitney, D. R. (1947). "On a test of whether one of two random variables is stochastically larger than the other". *Annals of Mathematical Statistics*, 18, 50-60.
- [21] Wilcoxon, F. (1945). Individual comparisons by ranking methods. *Biometrics*, 1, 80-83.
- [22] Dataxiom Software, Inc., 2001. *User's Guide StatMost Statistical Analysis and Graphics*. Fourth Edition. Dataxiom Software, Inc., (<http://www.dataxiom.com>)
- [23] Zhao, X., X. Zhang, T. Chi, H.Chen and Y. Miao. 2007. Flood simulation and emergency management: a web-based decision support system. *Proceedings of the 2nd IASME / WSEAS International Conference on Water Resources, Hydraulics & Hydrology*, Portoroz, Slovenia, May 15-17, 2007.
- [24] Liao, H. Y., T. H. Chang, A. P. Wang and B. W. Cheng, 2008. Fuzzy comprehensive assessment of typhoon flood. *WSEAS Transactions On Environment And Development*, Issue 3, Vol. 4: 257-266.

Table 1. Average Rainfall statistics by storm type for 62 storms between August 2006 and August 2007.

Type of Storm	Number of Storms	Storm start	Storm end	Storm Duration (hr)	n	Total Average Storm Rainfall (mm)	Standard Deviation (mm)	Maximum (mm)	Minimum (mm)
Localized	22	15:18	18:16	2.97	14	15.37	12.09	29.11	4.57
Upper Westerly trough	16	15:22	17:59	2.63	12	14.41	13.23	29.18	4.63
Tropical Easterly Wave	11	14:41	16:10	1.47	17	17.23	10.77	31.62	5.54
Cold Front	6	14:59	16:50	1.85	12	9.04	6.09	21.57	0.70
Tropical Westerly trough	6	13:31	17:39	4.14	17	27.03	9.66	41.90	6.53
Localized with cold front	1	15:51	17:40	1.82	13	13.64	NA	32.60	1.80
Overall Average	62	15:01	17:37	2.60	14	15.98	10.37	30.23	4.48

n stands for sample size or the number of operational rain gauges.

Table 2. Results of statistical comparisons between storms totals for all combinations of 16 rain gauges.

Statistical Analysis	Data Transformation	Percent of rain gauge pairs showing significant difference (%)
Mann-Whitney	None	25.0
Mann-Whitney	Log	21.6
Wilcoxon	None	17.0
Wilcoxon	Log	20.0
Average		20.9